BIOCHEMISTRY
including biophysical chemistry & molecular biology

Article

pubs.acs.org/biochemistry

Peroxisome Proliferation-Activated Receptor δ Agonist GW0742 Interacts Weakly with Multiple Nuclear Receptors, Including the Vitamin D Receptor

Premchendar Nandhikonda,[†] Adam Yasgar,[∥] Athena M. Baranowski,[†] Preetpal S. Sidhu,[†] Megan M. McCallum,[†] Alan J. Pawlak,[†] Kelly Teske,[†] Belaynesh Feleke,[†] Nina Y. Yuan,[†] Chinedum Kevin,[†] Daniel D. Bikle,[‡] Steven D. Ayers,[§] Paul Webb,[§] Ganesha Rai,[∥] Anton Simeonov,[∥] Ajit Jadhav,[∥] David Maloney,[∥] and Leggy A. Arnold*[,†]

[†]Department of Chemistry and Biochemistry, University of Wisconsin—Milwaukee, Milwaukee, Wisconsin 53211, United States

[‡]Endocrine Research Unit, Department of Medicine, Veterans Affairs Medical Center, San Francisco, California 94121, United States

[§]The Methodist Hospital Research Institute, Houston, Texas 77030, United States

[∥]NIH Chemical Genomics Center, National Human Genome Research Institute, National Institutes of Health, Bethesda, Maryland 20892-3370, United States

Supporting Information

ABSTRACT: A high-throughput screening campaign was conducted to identify small molecules with the ability to inhibit the interaction between the vitamin D receptor (VDR) and steroid receptor coactivator 2. These inhibitors represent novel molecular probes for modulating gene regulation mediated by VDR. Peroxisome proliferator-activated receptor (PPAR) δ agonist GW0742 was among the identified VDR−coactivator inhibitors and has been characterized herein as a pan nuclear receptor antagonist at concentrations of >12.1 μM. The highest antagonist activity for GW0742 was found for VDR and the androgen receptor. Surprisingly, GW0742 behaved as a PPAR agonist and antagonist, activating transcription at lower concentrations and inhibiting this effect at higher concentrations. A unique spectroscopic property of GW0742 was identified as well. In the presence of rhodamine-derived molecules, GW0742 increased the fluorescence intensity and level of fluorescence polarization at an excitation wavelength of 595 nm and an emission wavelength of 615 nm in a dose-dependent manner. The GW0742-inhibited NR−coactivator binding resulted in a reduced level of expression of five different NR target genes in LNCaP cells in the presence of agonist. Especially VDR target genes *CYP24A1*, *IGFBP-3*, and *TRPV6* were negatively regulated by GW0742. GW0742 is the first VDR ligand inhibitor lacking the secosteroid structure of VDR ligand antagonists. Nevertheless, the VDR-meditated downstream process of cell differentiation was antagonized by GW0742 in HL-60 cells that were pretreated with the endogenous VDR agonist 1,25-dihydroxyvitamin D_3.

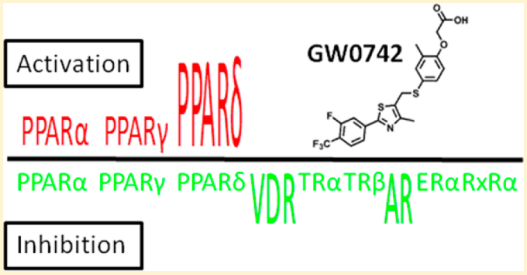

Nuclear receptor (NR) ligands represent one of the largest classes of currently FDA-approved drugs for a wide variety of human diseases.[1] The 48 identified members of this superfamily of transcription factors share a similar protein structure and bind, in the case of the steroid hormone receptors, to endogenous ligands with a similar steroid structure.[2] During the past decade, many new synthetic NR ligands with diverse scaffolds have been introduced, especially for peroxisome proliferation-activated receptors α (3363 ligands), γ (3891 ligands), and δ (1729 ligands).[3] Although the structural optimization of the NR ligand has been guided by affinity for a given NR, it is generally accepted that ligand selectivity among NRs has to be optimized as well to reduce side effects. The discovery that NR−coactivator binding is required for NR-mediated transcription led to a more stringent concept of selectivity for NR ligands.[4,5] NR ligand drug candidates should not only selectively bind to a certain NR but also selectively modulate the recruitment of particular nuclear receptor coactivators.[6] Many NR ligands with improved selectivity have been recently introduced, but the sheer number of NRs and affiliated coactivators that govern their specific gene regulation pattern has complicated the selectivity assessment of these ligands.[7]

A new concept for selectively modulating NR function involves the development of small molecules that directly inhibit the interaction between NRs and coregulators instead of interacting with the receptor ligand binding pocket to allosterically modulate interactions of the receptor with its target proteins.[8] The development of an inhibitor selective toward a particular coregulator−NR interaction could be highly

Received: March 12, 2013
Revised: April 24, 2013
Published: May 29, 2013

useful for the vitamin D receptor (VDR).[9] VDR binds to its endogenous ligand, 1,25-dihydroxyvitamin D_3 [1,25-$(OH)_2D_3$], with high affinity,[10] mediating changes in the transcription of genes responsible for cell differentiation, proliferation, and calcium homeostasis.[11] On the basis of its biological function, the VDR has been identified as an important pharmaceutical target for the treatment of metabolic disorders, skin diseases, cancer, autoimmune diseases, and cardiovascular diseases.[12] VDR, similar to other NRs, contains several functional domains, including a ligand binding domain (VDR-LBD), which mediates ligand-dependent gene regulation.[13] VDR binds DNA as a heterodimer with the retinoid X receptor (RXR).[14] In the unliganded state, VDR is associated with corepressor proteins, which repress transcription of VDR target genes.[15] In the presence of 1,25-$(OH)_2D_3$, the VDR-LBD undergoes a conformational change that prevents corepressor binding and permits interactions with coactivators, resulting in the formation of a multiprotein complex responsible for VDR-mediated transcription.[16]

VDR agonists have been developed for the treatment of metabolic bone diseases and proliferative skin disorders.[12] In contrast to the large number of reported VDR agonists, only a limited number of VDR ligand antagonists with the ability to allosterically inhibit the interactions between VDR and its coactivators have been described.[17−24] All of these antagonists are based on the secosteroid structure of 1,25-$(OH)_2D_3$. Mita et al. introduced the first reversible small molecule direct inhibitors of VDR−coactivator interactions with moderate NR selectivity.[25] The reported compounds inhibited both VDR-mediated and estrogen receptor β-mediated transcription. Recently, we reported the first irreversible direct inhibitors of the VDR−coactivator interaction.[26] This new class of compounds selectively inhibited the interaction between VDR and coactivator SRC2[27] among six other NR−coactivator interactions tested and reduced the level of expression of VDR target gene *TRPV6* in DU-145 prostate cancer cells in the presence of 1,25-$(OH)_2D_3$.

Herein, we describe the evaluation of compound GW0742, which was identified during a high-throughput screen (HTS) to identify small molecules that inhibit the interaction between VDR and nuclear receptor SRC2. GW0742 was introduced by GlaxoSmithKline in 2003 as a highly selective agonist for peroxisome proliferator-activated receptor δ (PPARδ).[28] Since then, GW0742 has been investigated in cell-based assays and *in vivo* to understand the role of PPARδ in hypertension,[29,30] diabetes,[31,32] inflammation,[33,34] obesity,[35] and cancer.[36−38] Interestingly, PPAR agonists have been shown to inhibit the transcription of VDR target gene CYP24A1 in the presence of 1,25-$(OH)_2D_3$.[39] The results presented herein show that GW0742, at micromolar concentrations, behaves as an antagonist of VDR and other nuclear receptors.

EXPERIMENTAL PROCEDURES

Reagents. 1,25-$(OH)_2D_3$ (calcitriol) was purchased from Endotherm. GW0742 was purchased from Tocris. Triiodothyronine (T3), GW7647, Rosiglitazone, dihydrotestosterone (DHT), Bexarotene, and estradiol were purchased from Sigma. LG190178 was synthesized using a published procedure.[40]

Labeled Coactivator Peptides. Peptides, such as SRC2-3 (CLQEKHRILHKLLQNGNSPA),[41] SRC2-2 (CEKHKILHRLLQDSS), and DRIP2 (CNTKNHPMLMNLLKDNPAQD), were purchased and labeled with cysteine-reactive fluorophores, such as fluorescein maleimides, Texas Red maleimides, and Alexa Fluor 647 maleimides, in a 50:50 DMF/PBS mixture. After purification by high-performance liquid chromatography, the corresponding labeled peptides were dissolved in DMSO and stored at −20 °C.

Protein Expression and Purification. The VDR-LBDmt DNA was kindly provided by D. Moras[42] and cloned into the pMAL-c2X vector (New England Biolabs). A detailed expression and purification protocol for VDR was reported previously.[41] Detailed expression and purification of protocols for PPARγ-LBD, TRβ-LBD, and AR-LBD were reported as well.[43]

High-Throughput FP Assay. HTS was conducted at the NIH Chemical Genomic Center. For details, see [AID:504847/pubchem].

VDR−SRC2-3 Inhibition Confirmation Assay. These assays were conducted in 384-well black polystyrene plates (Corning) using a buffer [25 mM PIPES (pH 6.75) 50 mM NaCl, 0.01% NP-40, 2% DMSO, VDR-LBD protein (0.6 μM), LG190178 (5 μM), and Alexa Fluor 647-labeled SRC2-3, Texas Red-labeled SRC2-3, or fluorescein-labeled SRC2-3 (7.5 nM) with optional 1 or 100 mM mercaptoethanol as indicated]. Small molecule transfer into a 20 μL assay solution was accomplished using a stainless steel pin tool (V&P Scientific), delivering 100 nL of a 10 mM compound solution. Fluorescence polarization was detected after 2 h at excitation and emission wavelengths of 650 and 665 nm (Alexa Fluor), 595 and 615 nm (Texas Red), and 495 and 520 nm (fluorescein), respectively. Three independent experiments were conducted in quadruplicate, and data were analyzed using nonlinear regression with a variable slope (GraphPad Prism).

VDR Ligand Competition Assay. Ligand antagonism was assessed by using a FP assay (PolarScreen, Invitrogen), which employs a rhodamine-labeled VDR ligand. Two independent experiments were conducted in quadruplicate, and data were analyzed using nonlinear regression with a variable slope (GraphPad Prism).

Transcription Assays. Briefly, HEK 293T cells (ATTC) were cultured in 75 cm^2 flasks using DMEM/High Glucose (Hyclone, catalog no. SH3024301), nonessential amino acids, HEPES (10 mM), penicillin and streptomycin, and 10% dialyzed FBS (Invitrogen, catalog no. 26400-044). At 70−80% confluency, 2 mL of untreated DMEM containing 1.56 μg of NR plasmid, 16 μg of a luciferase reporter gene, Lipofectamine LTX (75 μL), and PLUS reagent (25 μL) was added. After 16 h, the cells were harvested with 0.05% trypsin (3 mL) (Hyclone, catalog no. SH3023601), added to 15 mL of DMEM/High Glucose (Hyclone, catalog no. SH3028401), nonessential amino acids, sodium pyruvate (1 mM), HEPES (10 mM), penicillin and streptomycin, and 2% charcoal-treated FBS (Invitrogen, catalog no. 12676-011), and spun down for 2 min at 1000 rpm. The cell were resuspended in the same medium and plated in sterile cell culture-treated black 384-well plates with an optical bottom (Nunc, catalog no. 142761) at a concentration of 15000 cells/well, which had been previously treated with a 0.25% solution of Matrigel (BD Bioscience, catalog no. 354234). After 2 h, plated cells were treated with small molecules in vehicle DMSO, followed by a 16 h incubation. The following NR agonists were used: 1,25-$(OH)_2D_3$ (10 nM), GW7647 (30 nM), Rosiglitazone (300 nM), GW0742 (50 nM), DHT (10 nM), Bexarotene (200 nM), T3 (10 nM), and estradiol (10 nM). Transcription was

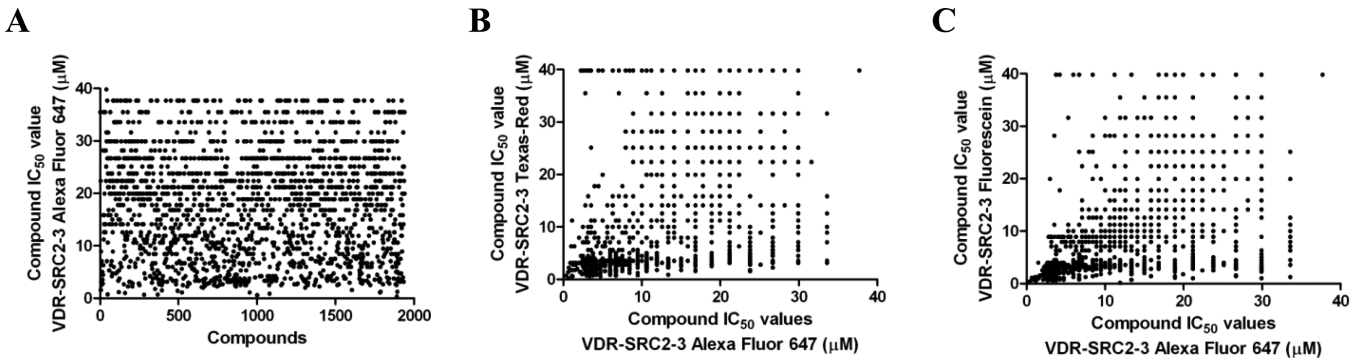

Figure 1. IC_{50} values of 1938 hit compounds using VDR-LBD and SRC2-3 labeled with (A) Alexa Fluor 647, (B) Texas Red in combination with Alexa Fluor 647, and (C) fluorescein in combination with Alexa Fluor 647.

assessed using Bright-Glo (Promega). Cell viability was assessed using CellTiter-Glo (Promega) for identically treated cells. Controls for cell viability were 3-dibutylamino-1-(4-hexylphenyl)propan-1-one (100 μM in DMSO) (positive) and DMSO (negative). Three independent experiments were conducted in quadruplicate, and data were analyzed using nonlinear regression with a variable slope (GraphPad Prism).

Western Blot of *in Vitro* Binding Reactions between SRC2 Bearing All Three NIDs and VDR-LBD in the Presence of GW0742. GST fusion proteins with SRC2 bearing all three NIDs were expressed in *Escherichia coli* BL21. Cultures were grown to an OD_{600} of 0.5−0.6 at 22 °C and induced with 0.5 mM isopropyl D-thiogalactoside for 12 h. The cultures were centrifuged (1000*g*), and bacterial pellets were resuspended in 20 mM Tris (pH 7.4), 200 mM NaCl, 1 mM NaN_3, 0.5 M EDTA, 1 mM DTT, and a protein inhibitor cocktail (Roche) and sonicated. Debris was pelleted by centrifugation (100000*g*). The supernatant was incubated with glutathione-Sepharose 4B beads (Amersham Biosciences) and washed. The protein on beads was stored with 10% glycerol at −20 °C. Each pull-down reaction was conducted in 100 μL of buffer [25 mM PIPES (pH 6.75), 50 mM NaCl, 0.01% NP-40, and 2% DMSO] using 100 nM calcitriol, 10 μM VDR-LBD-MPB, and GW0742. After 2 h at room temperature, 15 μL of SRC2 beads was added to each reaction mixture followed by a 30 min incubation. The reaction mixture was filtered, washed with buffer (100 μL), and eluted from the bead using a buffer and 10 mM reduced glutathione. Separation was conducted using sodium dodecyl sulfate−polyacrylamide gel electrophoresis followed by Western blotting using standard procedures with anti-MBP (E8032S, New England BioLabs) and anti-mouse IgG-Tr (sc-2781, Santa Cruz).

Semiquantitative Real-Time Polymerase Chain Reaction (RT-PCR). Briefly, LNCaP cells (ATTC) were cultured in 75 cm^2 flasks using DMEM/High Glucose (Hyclone, catalog no. SH3024301), nonessential amino acids, HEPES (10 mM), penicillin and streptomycin, and 10% dialyzed FBS (Invitrogen, catalog no. 26400-044). LNCaP cells were incubated at 37 °C with GW0742 (20 μM) in the presence or absence of DHT (10 nM), Rosiglitazone (5 μM), triiodothyronine (10 nM), or 1,25-$(OH)_2D_3$ (10 nM) for 18 h in a six-well plate. Cells of each well were harvested using 0.3 mL of 0.05% trypsin (Hyclone, catalog no. SH3023601) and added to DMEM (1 mL). The cell suspension was spun down for 2 min at 1000 rpm; the medium was removed, and the cell pellet was resuspended in RTL buffer (RNAeasy kit, Qiagen) with the addition of mercaptoethanol. The cells were lysed using a QIAshredder (Qiagen), and total RNA was isolated using an RNAeasy kit (Qiagen). A QuantiFast SYBR Green RT-PCR kit (Qiagen) was used for RT-PCR following the manufacturer's recommendations. The following primers were used: GAPDH FP, 5′-accacagtccatgccatcac-3′; GAPDH RP, 5′-tccaccaccctgttgctgta-3′; TRPV6 FP, 5′-ACTGTCATTGGGGCTATCATC-3′; TRPV RP, 5′-CAGCAGAATCGCATCAGGTC-3′; IGFBP3 FP, 5′-CGCCAGCTCCAGGAAATG-3′; IGFBP3 RP, 5′-GCATGCCCTTTCTTGATGATG-3′; UGT1A1 FP, 5′-GCCATGCAGCCTGGAATT-3′; UGT1A1 RP, 5′-GGCCTGGGCACGTAGGA-3′; PSA FP, 5′-TCTGCCTTTGTCCCCTAGAT-3′; PSA RP, 5′-AACCTTCATTCCCCAGGACT-3′; BTG2 FP, 5′-AGGGTAACGCTGTCTTGTGG-3′; BTG2 RP, 5′-TACAGTTCCCCAGGTTGAGG-3′; ANGPTL4 FP, 5′-AGGGTAACGCTGTCTTGTGG-3′; ANGPTL4 FP, 5′-TACAGTTCCCCAGGTTGAGG-3′. RT-PCR was conducted on a Mastercycler (Eppendorf). We used the ΔΔCt method to measure the fold change in the level of gene expression of target genes. Standard errors of the mean were calculated from four biological independent experiments performed in triplicate.

HL-60 Differentiation Assay. HL-60 cells (ATTC) were cultured in 75 cm^2 flasks using RPMI-1640 (ATTC, catalog no. 30-2001), nonessential amino acids, penicillin and streptomycin, and 10% dialyzed FBS (Invitrogen, catalog no. 26400-044). The cells were treated with 1,25-$(OH)_2D_3$ (50 nM) or vehicle DMSO and plated at a concentration of 2 M cells/mL in 384-well plates with an optical bottom (Nunc 142761). Cells were incubated with different concentrations of GW0742 for 4 days at 37 °C; 4 μL of nitro blue tetrazolium chloride (5.4 mg/mL) and phorbol 12-myristate 13-acetate (PMA) (100 μg/mL) was added to each well and incubated for 30 min at 37 °C. The amount of oxidized nitro blue tetrazolium was quantified at a wavelength of 550 nm applying a 4 × 4 scan of the full well area using the Tecan M1000 instrument. Two independent experiments were conducted in quadruplicate, and data were analyzed using nonlinear regression with a variable slope (GraphPad Prism).

RESULTS

A small molecule screen of ∼390000 compounds at different concentrations was conducted in 1536-well black polystyrene plates using fluorescence polarization (FP) [AID:504847/pubchem]. HTS identified inhibitors of the interaction between VDR and fluorescently labeled peptide SRC2-3, representing the NR interaction domain of steroid receptor coactivator 2 (SRC2). The screen was conducted in the presence of VDR-LBD protein (800 nM), VDR agonist LG190178[40] (5 μM), and

dx.doi.org/10.1021/bi400321p | *Biochemistry* 2013, 52, 4193−4203

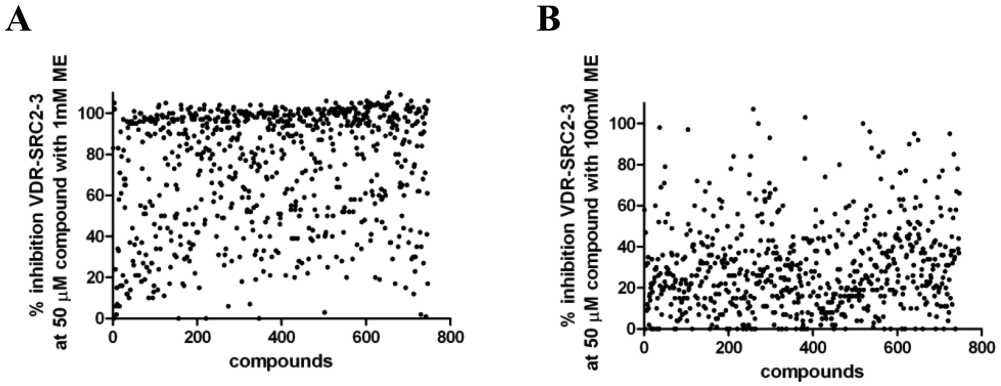

Figure 2. Inhibition for the VDR−SRC2-3 Alexa Fluor 647 interaction by small molecules (50 μM) in the presence of 1 or 100 mM 2-mercaptoethanol (ME).

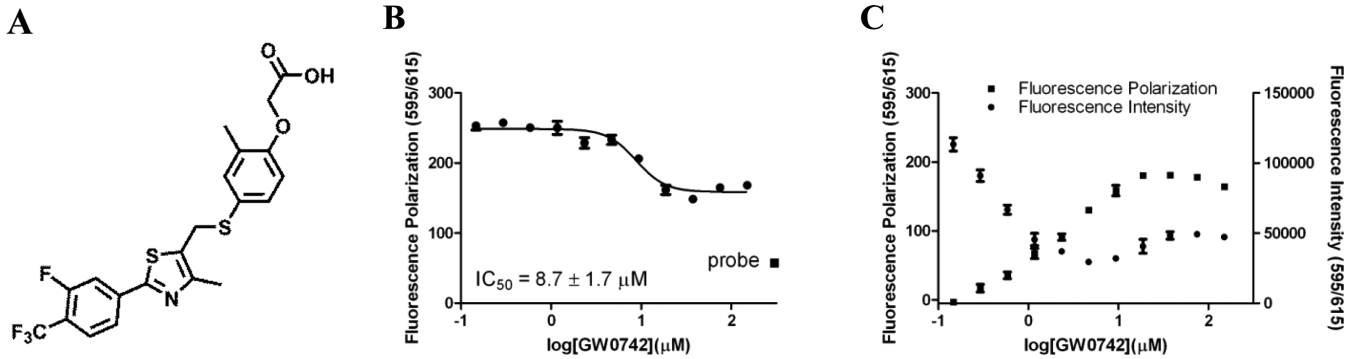

Figure 3. VDR−GW0742 interactions. (A) Chemical structure of GW0742. (B) FP VDR ligand competition assay. (C) Fluorescence interaction between GW0742 and the rhodamine-labeled VDR ligand.

Alexa Fluor 647-labeled coregulator peptide SRC2-3 (7.5 nM). Fluorescence polarization was detected at an emission wavelength at 650 nm and an excitation wavelength of 665 nm; 1938 compounds exhibited IC_{50} values of ≤40 μM in the primary screen (Figure 1A). Furthermore, these compounds were validated with two alternative FP assays employing Texas Red-labeled SRC2-3 (excitation and emission at 595 and 615 nm, respectively) [AID:602201/pubchem] and fluorescein-labeled SRC2-3 (excitation and emission at 495 and 520 nm, respectively) [AID:602200/pubchem] (Figure 1B,C).

Further characterization of the 1938 initial hits revealed that 69% of the compounds exhibited IC_{50} values of ≤40 μM in the FP assay employing VDR-LBD and Texas Red-labeled SRC2-3 (Figure 1B). A good correlation between compound activities in this assay and validation assays was observed. 83% of the 1938 hit compounds also exhibited IC_{50} values of ≤40 μM in the FP assay employing Fluorescein-labeled SRC2−3 (Figure 1C). Also in this case, a good correlation with the assay employing SRC2-3 and Alexa Fluor 647 was observed.

On the basis of these results, 747 compounds were selected with an emphasis on diverse scaffolds and functionality. To delineate compounds that might inhibit coactivator binding by irreversibly reacting with cysteine residues of the VDR-LBD protein, the VDR−SRC2-3 FP assay was conducted in the presence of 1 or 100 mM 2-mercaptoethanol (ME). The hypothesis here is that electrophilic compounds are more likely to react in the presence of excess nucleophilic ME than with protein nucleophilic protein residues such as cysteine. We introduced this method for the electrophilic compound DHPPA, which showed a reduced level of thyroid receptor binding in the presence of 100 mM ME.[44] The results of both assays are depicted in Figure 2.

Interestingly, we observed a significant reduction in the ability of the majority of compounds to inhibit the interaction between VDR and SRC2-3 in the presence of 100 mM ME in comparison with that in the presence of 1 mM ME (Figure 2B). This suggests that a large number of our initial hits may inhibit VDR−coactivator interactions via modification of surface cysteine residues. However, activities of a significant minority of compounds were not influenced by a higher concentration of ME (100 mM), and among these was GW0742 (Figure 3A).

The following activities were measured for GW0742 during the HTS campaign: (1) VDR−SRC2-3 inhibition (FP assays) (IC_{50} values), 14 μM (Alexa Fluor 647), 25.1 μM (fluorescein), and inconclusive (Texas Red); (2) VDR transcription assay (VDR-GeneBLAzer, Invitrogen), IC_{50} value of 26 μM at a maximal response of 30% as defined by the absence of VDR agonist 1,25-$(OH)_2D_3$ [AID:602202, pubchem]; (3) toxicity in HEK293T cells (CellTiter-Glo, Promega), 18% cell death at a concentration of 45.8 μM [AID:602204, pubchem].

To determine that GW0742 is interacting with VDR and not the coactivator, a commercially available VDR ligand binding FP assay was used employing VDR and a rhodamine-labeled VDR ligand (Figure 3B).

Using increasing concentrations of GW0742, competition of VDR−ligand binding was confirmed with an IC_{50} value of 8.7 ± 1.7 μM. Interestingly, partial inhibition was observed with respect to 100% free probe (55 mP) measured in the absence of VDR [Figure 3B (■)]. Prompted by this result and by the fact that the FP assay employing Texas Red-labeled SRC2-3 was inconclusive during the HTS campaign, we analyzed the

dx.doi.org/10.1021/bi400321p | Biochemistry 2013, 52, 4193−4203

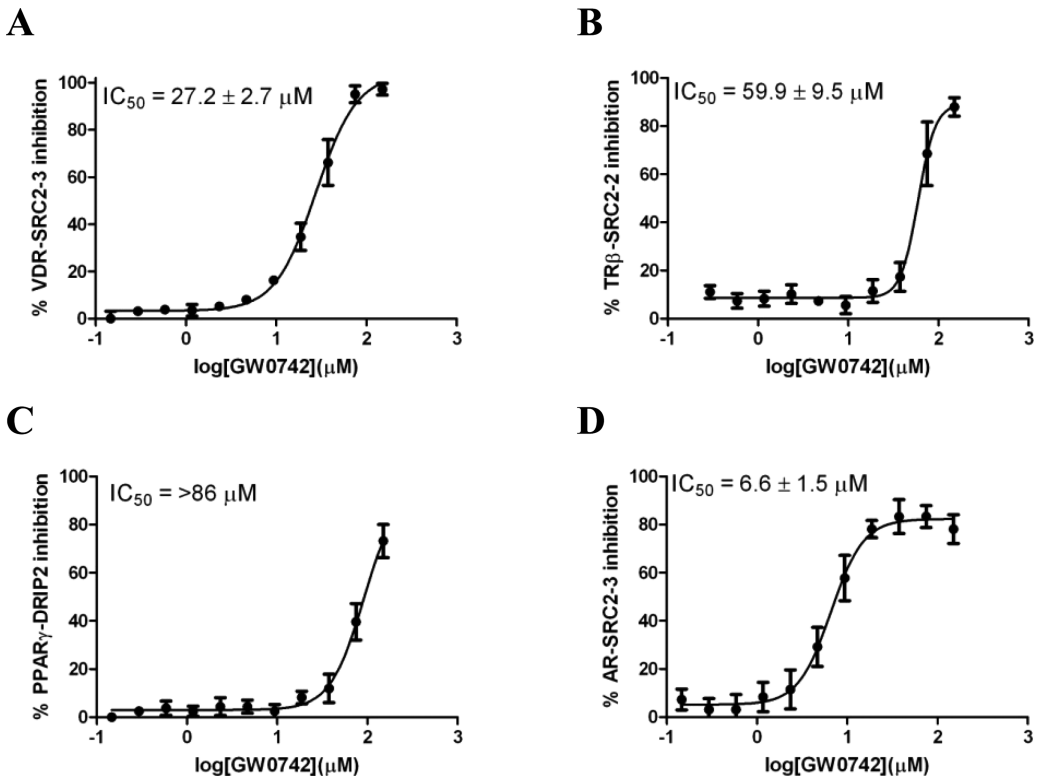

Figure 4. Summary of nuclear receptor−coactivator inhibition in the presence of GW0742 using FP. (A) Inhibition of the VDR−SRC2-3 interaction. (B) Inhibition of the TRβ−SRC2-2 interaction. (C) Inhibition of the PPARγ−DRIP2 interaction. (D) Inhibition of the AR−SRC2-3 interaction. The conditions for different NRs were as follows. VDR-LBD (0.8 μM), Alexa Fluor 647-labeled SRC2-3 (7 nM), and LG190178 (2 μM); TRβ-LBD (1 μM), Alexa Fluor 647-labeled SRC2-2 (7 nM), and triiodothyronine (10 nM); PPARγ-LBD (5 μM), Alexa Fluor 647-labeled DRIP2 (7 nM), and Rosiglitazone (5 μM); and AR-LBD (5 μM), Alexa Fluor 647-labeled SRC2-3 (7 nM), and dihydrotestosterone (10 nM) were incubated with GW0742 for 2 h.

interaction between GW0742 and the rhodamine-labeled VDR ligand in the absence of VDR (Figure 3C). Surprisingly, we found that both fluorescence intensity and fluorescence polarization of the rhodamine-labeled VDR ligand increased at higher GW0742 concentrations. Similar results were found for Texas Red-labeled SRC2-3 in the presence of GW0742 using the same excitation and emission wavelengths (results not shown). GW0742 by itself showed no significant fluorescence under these conditions. On the basis of these results, we concluded that GW0742 inhibited the interaction between VDR and rhodamine-labeled VDR ligand, but that IC_{50} values measured with Alexa Fluor 647-labeled SRC2-3 are a more reliable measure of the inhibitory activity of the ligand. No change in fluorescence intensity and fluorescence polarization was detected at an emission wavelength at 650 nm and an excitation wavelength of 665 nm for Alexa Fluor 647-labeled SRC2-3 and increasing concentrations of GW0742 (results not shown). In addition, we investigated the interaction between GW0742 and SRC2 using isothermal titration calorimetry (ITC), but no specific interaction was observed (Supporting Information).

FP assays were conducted to determine the selectivity of GW0742 with respect to its ability to inhibit the interaction between other nuclear receptors and Alexa Fluor 647-labeled coactivator peptides. These included VDR and SRC2-3, thyroid hormone receptor β (TRβ) and SRC2-2, peroxisome proliferation-activated receptor γ (PPARγ) and DRIP2, derived from coactivator DRIP205,[45] and AR and SRC2-3. The results are depicted in Figure 4.

The inhibition of VDR−SRC2-3 binding in the presence of GW0742, demonstrated during the HTS campaign, was confirmed with a calculated IC_{50} value of 27.2 ± 2.7 μM (Figure 4A). The ability of GW0742 to disrupt the TR−SRC2-2 and PPARγ−DRIP2 interactions was modest with IC_{50} values of 59.9 ± 9.5 and >86 μM, respectively (Figure 4B,C). The strongest GW0742 inhibition was observed for the AR−SRC2-3 interaction with an IC_{50} value of 6.6 ± 1.5 μM (Figure 4D).

Many other groups have investigated GW0742 with respect to different nuclear receptor binding using a variety of assays. These include PPARα, PPARγ, and PPARδ using cell-based transactivation assays (alkaline phosphatase as the reporter enzyme), where GW0742 exhibited agonistic EC_{50} values of 1.1 ± 0.109 μM (PPARα), 2.0 ± 1.3 μM (PPARγ), and 0.001 ± 0.002 μM (PPARδ).[28] Antagonistic activity of GW0742 was also observed in HTS campaigns using GeneBLAzer assays (Invitrogen) employing estrogen receptor α (ERα, AID:588513, pubchem), the glucocorticoid receptor (GR, AID:588533, pubchem), PPARδ (AID:588535, pubchem), PPARγ (AID588537, pubchem), the retinoid X receptor (RxR, AID:588546, pubchem), and TRβ (AID:588547, pubchem). The activity of GW0742 found for the majority of these nuclear receptors was in the micromolar range and exhibited inconclusive dose−response curves in most cases.

Therefore, an array of nuclear receptor-mediated transcription assays was used to confirm the pan nuclear receptor−coactivator inhibition caused by high concentrations of GW0742 in the FP assay. For VDR, TRα, and TRβ, HEK293T cells were transfected with the nuclear receptor

dx.doi.org/10.1021/bi400321p | *Biochemistry* 2013, 52, 4193−4203

expression vector and luciferase reporter under control of the cognate nuclear receptor response elements or target gene promoters. For all other nuclear receptors, one-hybrid assays employing nuclear receptor LBDs fused to the DNA binding domain (DBD) of GAL4 and a luciferase reporter plasmid driven by five copies of the GAL4 binding site fused to a *tk* promoter were employed. The assays were conducted in 384-well plates, and the amount of luciferase formed was quantified after 18 h using Bright-Glo. The transcription assays were conducted in the presence and absence of endogenous ligands or synthetic agonists using different GW0742 concentrations. The EC_{50} and IC_{50} values are summarized in Table 1.

Table 1. Evaluation of GW0742 in Different Nuclear Receptor Reporter Assays

entry	nuclear receptor	agonist EC_{50} (μM)[k]	antagonist IC_{50} (μM)[k]
1	VDR	*j*	14.7 ± 1.5[a]
2	PPARα	1.3 ± 0.3	37.4 ± 8.2[b]
3	PPARγ	2.8 ± 0.7	20.2 ± 5.4[c]
4	PPARδ	0.0037 ± 0.0014	21.6 ± 4.9[d]
5	AR	*j*	12.1 ± 5.3[e]
6	RxRα	*j*	22.9 ± 3.8[f]
7	TRα	*j*	31.4 ± 4.0[g]
8	TRβ	*j*	25.8 ± 5.2[h]
9	ERα	*j*	21.3 ± 7.2[i]

[a] 1,25-$(OH)_2D_3$ (10 nM). [b] GW7647 (30 nM). [c] Rosiglitazone (300 nM). [d] GW0742 (50 nM). [e] DHT (10 nM). [f] Bexarotene (200 nM). [g] T3 (10 nM). [h] T3 (10 nM). [i] Estradiol (10 nM). [j] No activation detected. [k] Three independent experiments were conducted in quadruplicate, and data were analyzed using nonlinear regression with a variable slope (GraphPad Prism).

As expected, GW0742 was able to activate transcription mediated by only PPARα, PPARγ, and PPARδ among the nuclear receptors tested. The measured EC_{50} values, 1.3 ± 0.3 μM for PPARα, 2.8 ± 0.7 μM for PPARγ, and 0.0037 ± 0.0014 μM for PPARδ (Table 1, entries 2−4), respectively, were in agreement with previously reported results.[28] In contrast, inhibition of transcription was found for all nuclear receptors within an IC_{50} value range of 12.1−37.4 μM. Interestingly, GW0742 exhibited significantly lower IC_{50} values for VDR and AR relative to other nuclear receptors with IC_{50} values of 12.1 and 14.7 μM, respectively (Table 1, entries 1 and 5, respectively). The cell viability in the presence of GW0742 was quantified under the same conditions using CellTiter-Glo (data not shown). At 37.5 μM GW0742, 93 ± 3% of the cell population was viable, and at 18.7 μM GW0742, no toxicity was observed. This observation is in agreement with the HTS data described previously.

For PPARs, GW0742 exhibited an agonistic effect at lower concentrations and an antagonistic effect at higher concentrations as shown for PPARγ for the FP assay (Figure 4) and transcription assay depicted in Figure 5. GW0742 EC_{50} values determined in both assays are very similar, 2.6 μM for the FP assay and 2.8 μM for transcription. At >20 μM GW0742, we observed significant PPARγ-mediated transcriptional inhibition (Figure 5B), whereas significant inhibition between PPARγ-LBD and DRIP2 was observed for GW0742 at higher concentrations (>86 μM).

GW0742 also inhibited the interaction between VDR-LBD and an SRC2 fragment bearing three nuclear interaction domains in a Western pull-down assay (Figure 6). Control experiments indicated that SRC2 binds to VDR in the presence of VDR ligand LG190178 (Figure 6, lane 8) but not in the absence of the ligand (Figure 6, lane 9). The faint bands in the absence of the ligand and VDR were caused by nonspecific binding of the VDR antibody to SRC2 beads. The VDR−SRC2 interaction was blocked in a dose-dependent manner by GW0742 (Figure 8, lanes 1−7). Although significant inhibition of the VDR−SRC2 interaction was observed at 80−120 μM GW0742, residual bands could still be detected partially because of unspecific binding of the VDR antibody to SRC2 beads as observed for the controls.

LNCaP cancer cells express different nuclear receptors, including AR,[46] PPARγ,[47] TRβ,[48] and VDR.[49] Furthermore, steroid receptor coactivators 1, 2, and 3 and DRIP205, essential for transcriptional activation, are expressed in these cells.[50,51] On the basis of these reports, we investigated the ability of GW0742 to inhibit nuclear receptor transcriptional activity by quantifying the RNA levels of different target genes in the presence and absence of endogenous or synthetic ligands (Figure 7).

For AR, expression of the UDP-glucuronosyltransferase 1 family polypeptide A cluster (*UGT1A1*)[52] and the prostate-specific antigene (*PSA*)[53] was upregulated in the presence of DHT (Figure 7A,B). LNCaP cells treated with DHT (10 nM) and 20 μM GW0742 showed a significant inhibitory effect. PPARγ target gene angiopoietin-related protein 4 (*FIAF/ANGPTL4*)[54] was induced by Rosiglitazone (5 μM), and this

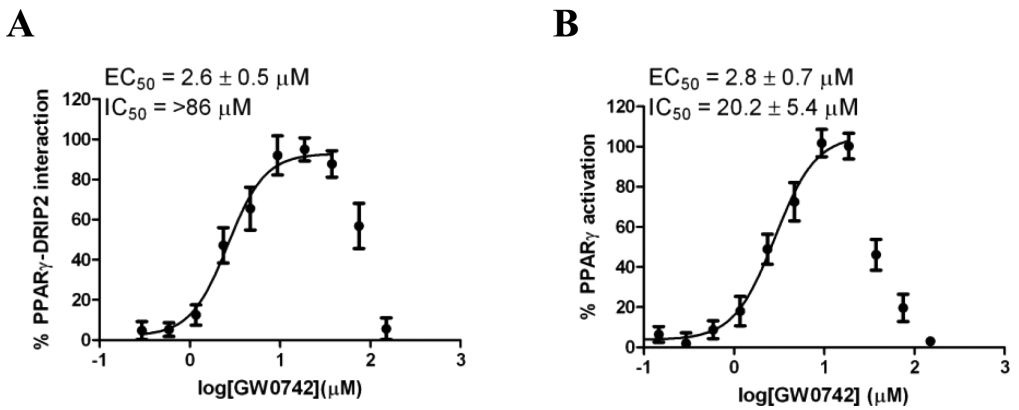

Figure 5. Agonistic and antagonistic effect of GW0742 with respect to PPARγ. (A) FP assay using PPARγ-LBD and Alexa Fluor 647-labeled DRIP2. (B) One-hybrid transcription assay employing PPARγ.

dx.doi.org/10.1021/bi400321p | *Biochemistry* 2013, 52, 4193−4203

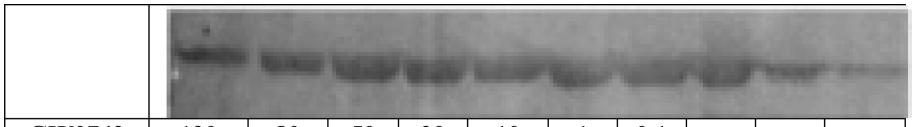

GW0742	120	80	50	20	10	1	0.1	-	-	-
VDR-LBD	+	+	+	+	+	+	+	+	+	-
SRC2	+	+	+	+	+	+	+	+	+	+
LG190178	+	+	+	+	+	+	+	+	-	-
lane	1	2	3	4	5	6	7	8	9	10

Figure 6. Inhibition of the VDR−SRC2 interaction by GW0742 analyzed by a Western pull-down assay.

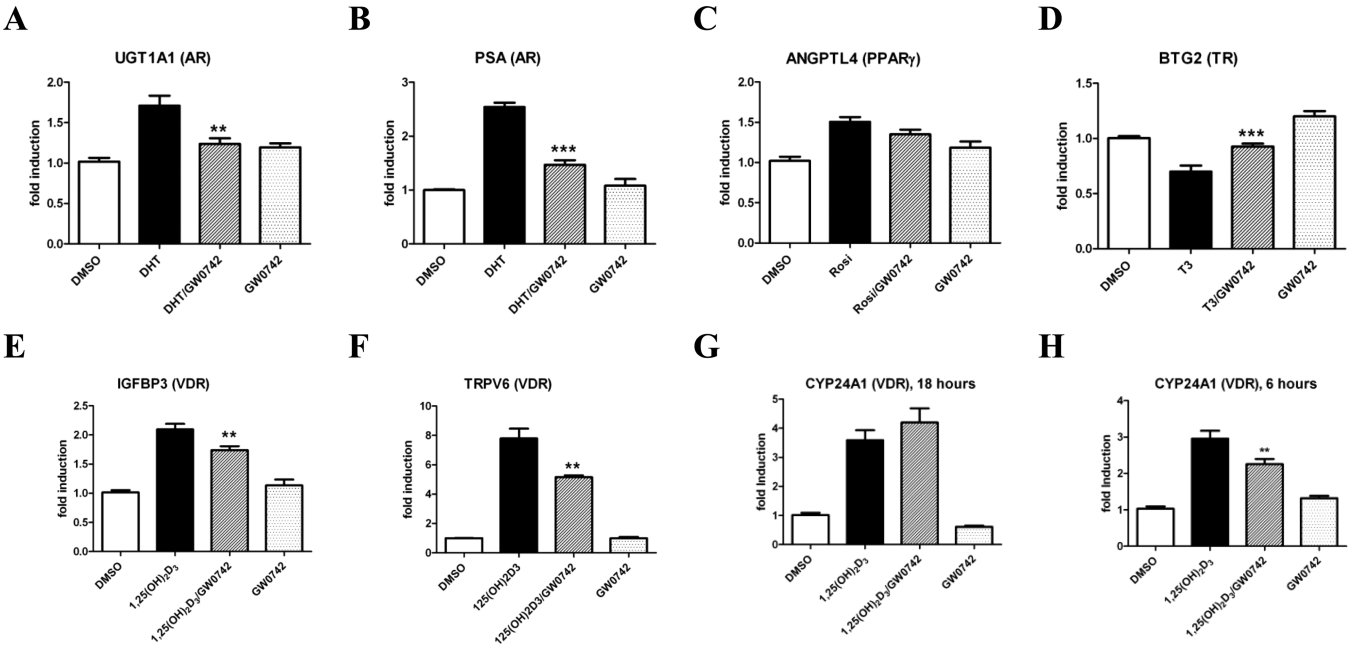

Figure 7. Gene regulation by GW0742 (20 μM; 50 μM for panel H) in LNCaP cells after 18 h (or as indicated) in the presence and absence of NR ligands: (A and B) DHT (10 nM), (C) Rosiglitazone (5 μM), (D) triiodothyronine (10 nM), and (E−H) 1,25-$(OH)_2D_3$ (10 nM). Standard errors of the mean were calculated from four biological independent experiments performed in triplicate. *P < 0.05. **P < 0.01. ***P < 0.001 (Student's t test).

response was unaffected by GW0742 (20 μM) (Figure 7C). TR target gene B-cell translocation gene 2 (BTG2)[55] was downregulated in the presence of T3 as shown in Figure 7D. This effect was reversed by GW0742 (20 μM), confirming the inhibitory action of GW0742 upon TR demonstrated in other assays. Finally, VDR target genes *IGFBP-3*[56,57] and *TRPV6*[58,59] (Figure 7E,F) were strongly induced by 1,25-$(OH)_2D_3$ (10 nM), and GW0742 selectively inhibited this effect. For VDR target gene CYP24A1,[60] we observed induction at 6 and 18 h in the presence of 1,25-$(OH)_2D_3$. Interestingly, only at the earlier time point of 6 h and 50 μM GW0742 was a significant inhibition of this induction found (Figure 7G,H).

As mentioned earlier, VDR governs expression of genes responsible for differentiation of human promyelocyte HL-60 cells into monocytes by 1,25-$(OH)_2D_3$.[61,62] VDR antagonists with a secosteroid structure inhibit this effect.[18,19,22] The established differentiation assay employs nitro blue tetrazolium chloride to colorimetrically quantify the amount of cellular superoxide in the presence of phorbol 12-myristate 13-acetate (PMA) that functions as a stimulant of the respiratory burst.[63] HL-60 cells were incubated for 4 days with and without 1,25-$(OH)_2D_3$ (10 nM) and GW0742 in a dose-dependent manner. The results are shown in Figure 8.

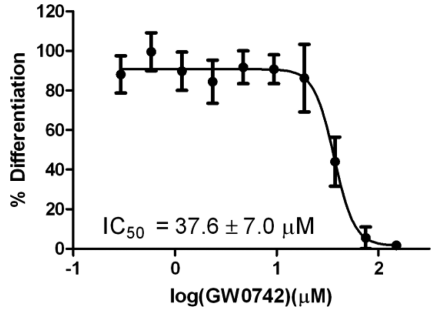

Figure 8. Inhibition of differentiation of HL-60 cells induced by 1,25-$(OH)_2D_3$ (50 nM) in the presence of GW0742.

A strong HL-60 cell differentiation was observed in the presence of 1,25-$(OH)_2D_3$. A significant reduction in the level of 1,25-$(OH)_2D_3$-induced differentiation was observed for GW0742 at concentration of >37.5 μM. Significant HL-60 cell death was observed at only 150 μM GW0742.

DISCUSSION

This study reports a successful HTS campaign for identifying new inhibitors of VDR−coactivator interaction. A novel

dx.doi.org/10.1021/bi400321p | Biochemistry 2013, 52, 4193−4203

strategy for delineating potential irreversible inhibitors, which are likely to react with a nucleophilic protein residue, from a pool of hit compounds was introduced by executing a secondary screen in the presence of a high concentration of the nucleophile ME. A ME concentration of 100 mM was essential in significantly reducing the number of hit compounds.

GW0742, a PPARδ agonist, was identified among the VDR−coactivator inhibitors that were not influenced by ME. Interestingly, GW0742 exhibited characteristics of a pan nuclear receptor antagonist at concentrations of >12.1 μM, as demonstrated for biochemical FP assays and cell-based transcription assays. While GW0742 inhibited the activity of a large number of nuclear receptors, albeit at micromolar concentrations, it inhibited VDR and AR activity most effectively. Interestingly, GW0742 also behaved as an agonist or antagonist for PPARα, PPARγ, and PPARδ, activating transcription at low concentrations and inhibiting this effect at higher concentrations.

The mechanism by which GW0742 inhibits activity of VDR and other nuclear receptors is not absolutely clear. Unexpectedly, we found that GW0742 inhibits the interaction between VDR and its small molecule ligand. While ligand competition appears to be incomplete, we suspect that our ligand binding assay underestimates the effectiveness of GW0742 competition because of an unexpected spectroscopic property of GW0742 discovered in this study. In the presence of rhodamine-derived compounds, an increase in fluorescence intensity was observed at higher GW0742 concentrations using an excitation wavelength of 595 nm and an emission wavelength of 615 nm. The interaction between GW0742 and the rhodamine compound also increases fluorescence polarization at the same excitation and emission wavelengths. This unusual spectroscopic behavior of GW0742 might partly mask its ability to compete with the fluorescent VDR agonist and could also represent an underlying reason for a number of false positive FP HTS hits. Thus, these data are suggestive of a conventional antagonist mode of action, in which GW0742 interacts with the VDR ligand binding site and allosterically disrupts the interaction between VDR and SRC2.

Results with PPARs, in which low concentrations of GW0742 display agonist behaviors and high concentrations inhibit this effect, suggest that other mechanisms may be at play. Similar behaviors have been reported for 4-hydroxytamoxifen (HT) with regard to estrogen receptors (ERs). A crystal structure of ERβ showed one HT molecule bound to the ligand binding site and another at the coactivator binding site.[64] As a result, ER was activated at low HT concentrations by ligand-induced conformational changes that allowed coactivator recruitment, but ER−coactivator interaction was inhibited at higher HT concentrations by competition for ER coactivator binding.[65] A similar mechanism might be one explanation for the agonist and/or antagonist behavior of GW0742 with regard to PPAR binding. There are other possibilities; PPARs possess large ligand binding pockets that can accommodate more than one ligand.[66] Thus, high GW0742 concentrations could result in unusual PPAR:ligand stoichiometries that could trigger inactive receptor conformations. Clarification of this issue will require further investigation.

Regardless of the mechanism of action, our studies revealed that GW0742 is effective in cell culture models. The therapeutic ratio (efficacy:toxicity) for GW0742 is relatively low for VDR-mediated processes (5:1) but very large for PPARδ (20000:1). The downstream effect of nuclear receptor−coactivator inhibition by GW0742 resulted in the suppression of VDR genes *IGFBP-3* and *TRPV6* in LNCaP cells in the presence of 1,25-$(OH)_2D_3$. Other than in the prostate, the proteins encoded by these genes are strongly expressed in the placenta.[67] Therefore, GW0742 treatments might be problematic during pregnancy. As observed by other groups, classic VDR target gene *CYP24A1* was moderately upregulated by 1,25-$(OH)_2D_3$ in LNCaP cells.[49] The inhibition of *CYP24A1* transcription induced by 50 μM GW0742 at only the earlier time point is likely caused by different levels of expression of CYP24A1 over time, which has been shown in PC-3 cells.[68] In addition, we found the inhibition of transcription of AR target genes *UGT1A1* and *PSA* in the presence of GW0742 in LNCaP upon stimulation with DHT. The proteins encoded by these genes are found at increased levels in patients with prostate cancer and prostatitis. Thus, GW0742 might have beneficial effects for both conditions. BTG2, a TRβ target gene, encodes coregulator BTG2, which has been shown to inhibit cell cycle progression at the G1 checkpoint by repressing cyclin D1 transcription.[69] In the presence of T3, BTG2 is downregulated in LNCaP cells but T3 suppression is inhibited in the presence of 20 μM GW0742. The regulation of PPAR target gene ANGPL4, which plays a significant role in fat metabolism, was inconclusive at the GW0742 concentration tested. *ANGPTL4* activation in the presence of Rosiglitazone and GW0742 was reported for HT29 colon cancer cells, although at a GW0742 concentration of 1 μM.[70] Thus, high local concentrations of GW0742 have a strong influence on the gene regulation mediated by PPARs and other nuclear receptors. The activation of transcription by 1,25-$(OH)_2D_3$ induces differentiation of HL-60 cells, a process that was shown to be inhibited by GW0742 in a dose-dependent manner. Overall, we have demonstrated the interactions between GW0742 and different NRs with diverse transcriptional and biological effects underlining the possibility that GW0742 might share a privileged scaffold recognized by many members of the NR superfamily. With respect to VDR, GW0742 is the first ligand antagonist lacking a secosteroid structure, which inhibits the transcriptional activation of VDR target genes in the presence of 1,25-$(OH)_2D_3$. Because of the fact that the three-dimensional folding of VDR and resulting interactions with coregulators are strongly dependent on the structure of the bound ligand,[71] we expect that GW0742 will exhibit different biological responses than the current secosteroid VDR antagonist. We are currently in the process of developing new VDR-selective antagonists based on GW0742 to determine the downstream effect of VDR−coactivator inhibition without influencing PPAR signaling.

■ ASSOCIATED CONTENT

Ⓢ Supporting Information

Absence of binding between GW0742 and SRC2 as determined using ITC. This material is available free of charge via the Internet at http://pubs.acs.org.

■ AUTHOR INFORMATION

Corresponding Author

*E-mail: arnold2@uwm.edu. Phone: (414) 229-2612. Fax: (414) 229-5530.

Author Contributions

P.N. and A.Y. contributed equally to this work.

Funding

This work was supported by the University of Wisconsin—Milwaukee (UWM) (L.A.A.), the UWM Research Growth Initiative (RGI Grant 2012) (L.A.A.), National Institutes of Health Grant R03DA031090 (L.A.A.), the UWM Research Foundation (Catalyst grant), the Lynde and Harry Bradley Foundation (L.A.A.), the Richard and Ethel Herzfeld Foundation (L.A.A.), and the Molecular Libraries Initiative of the National Institutes of Health Roadmap for Medical Research (Grant U54MH084681) (G.R., A.S., A.J., A.Y., and D.M.).

Notes

The authors declare no competing financial interest.

■ ACKNOWLEDGMENTS

We thank Robin Goy and Nicholas Nassif for the production of the VDR protein.

■ ABBREVIATIONS

VDR, vitamin D receptor; NR, nuclear hormone receptor; FP, fluorescence polarization; SRC2, steroid receptor coactivator 2; SRC2-3, third NR interaction domain of the steroid receptor coactivator 2 peptide; *TRPV6*, transient receptor potential vanilloid type 6 gene; *CYP24A1*, 1,25-dihydroxyvitamin D_3 24-hydroxylase; 1,25-$(OH)_2D_3$, 1,25-dihydroxyvitamin D_3; DBD, DNA binding domain; LBD, ligand binding domain; RxR, retinoid X receptor; HTS, high-throughput screening; DMSO, dimethyl sulfoxide; HEK293T, human embryonic kidney; AR, androgen receptor; ERα, estrogen receptor α; TRβ, thyroid receptor β; PPARα, peroxisome proliferator-activated receptor α; PPARγ, peroxisome proliferator-activated receptor γ; PPARδ, peroxisome proliferator-activated receptor δ; DRIP205, VDRR-interacting protein 205; GST, glutathione *S*-transferase; GAPDH, glyceraldehyde-3-phosphate dehydrogenase; NCGC, NIH Chemical Genomic Center; ME, mercaptoethanol; T3, triiodothyronine; DHT, dihydrotestosterone; GAL4, yeast transcription activator protein GAL4; HT, 4-hydroxytamoxifen; *UGT1A1*, UDP-glucuronosyltransferase 1 family polypeptide A cluster; *PSA*, prostate-specific antigene; *ANGPTL4*, angiopoietin-related protein 4; *BTG2*, B-cell translocation gene 2; *IGFBP-3*, insulin-like growth factor binding protein; HL-60, human promyelocytic leukemia; PMA, phorbol 12-myristate 13-acetate; DMF, dimethylformamide; PBS, phosphate-buffered saline; PIPES, piperazine-*N*,*N*′-bis(2-ethanesulfonic acid); NP-40, Tergitol-type NP-40; HEPES, 4-(2-hydroxyethyl)-1-piperazineethanesulfonic acid; FBS, fetal bovine serum; DMEM, Dulbecco's modified Eagle's medium; NID, nuclear receptor interaction domain; EDTA, ethylenediaminetetraacetic acid; DTT, dithiothreitol; MBP, maltose binding protein; LNCaP, human prostate cancer cells.

■ REFERENCES

(1) Overington, J. P., Al-Lazikani, B., and Hopkins, A. L. (2006) How many drug targets are there? *Nat. Rev. Drug Discovery 5*, 993−996.

(2) Bain, D. L., Heneghan, A. F., Connaghan-Jones, K. D., and Miura, M. T. (2007) Nuclear receptor structure: Implications for function. *Annu. Rev. Physiol. 69*, 201−220.

(3) The Binding Database (2013) ChemAxon.

(4) Ding, X. F., Anderson, C. M., Ma, H., Hong, H., Uht, R. M., Kushner, P. J., and Stallcup, M. R. (1998) Nuclear receptor-binding sites of coactivators glucocorticoid receptor interacting protein 1 (GRIP1) and steroid receptor coactivator 1 (SRC-1): Multiple motifs with different binding specificities. *Mol. Endocrinol. 12*, 302−313.

(5) Voegel, J. J., Heine, M. J., Tini, M., Vivat, V., Chambon, P., and Gronemeyer, H. (1998) The coactivator TIF2 contains three nuclear receptor-binding motifs and mediates transactivation through CBP binding-dependent and -independent pathways. *EMBO J. 17*, 507−519.

(6) McKenna, N. J., and O'Malley, B. W. (2001) Nuclear receptors, coregulators, ligands, and selective receptor modulators: Making sense of the patchwork quilt. *Ann. N.Y. Acad. Sci. 949*, 3−5.

(7) O'Malley, B. W., Malovannaya, A., and Qin, J. (2012) Minireview: Nuclear Receptor and Coregulator Proteomics—2012 and Beyond. *Mol. Endocrinol. 26*, 1646−1650.

(8) Moore, T. W., and Katzenellenbogen, J. A. (2009) Inhibitors of Nuclear Hormone Receptor/Coactivator Interactions. *Annu. Rep. Med. Chem. 44*, 443−457.

(9) Bikle, D. D., Teichert, A., Arnold, L. A., Uchida, Y., Elias, P. M., and Oda, Y. (2010) Differential regulation of epidermal function by VDR coactivators. *J. Steroid Biochem. Mol. Biol. 121*, 308−313.

(10) Brumbaugh, P. F., and Haussler, M. R. (1974) 1α,25-Dihydroxycholecalciferol receptors in intestine. I. Association of 1α,25-dihydroxycholecalciferol with intestinal mucosa chromatin. *J. Biol. Chem. 249*, 1251−1257.

(11) Jurutka, P. W., Whitfield, G. K., Hsieh, J. C., Thompson, P. D., Haussler, C. A., and Haussler, M. R. (2001) Molecular nature of the vitamin D receptor and its role in regulation of gene expression. *Rev. Endocr. Metab. Disord. 2*, 203−216.

(12) Feldman, D., Pike, J. W., and Glorieux, F. H. (2005) *Vitamin D*, 2nd ed., Vols. *1*−*2*, Elsevier, Burlington, MA.

(13) Yamada, S., Shimizu, M., and Yamamoto, K. (2003) Vitamin D receptor. *Endocr. Dev. 6*, 50−63.

(14) Toell, A., Polly, P., and Carlberg, C. (2000) All natural DR3-type vitamin D response elements show a similar functionality in vitro. *Biochem. J. 352* (Part2), 301−309.

(15) Kim, J. Y., Son, Y. L., and Lee, Y. C. (2009) Involvement of SMRT corepressor in transcriptional repression by the vitamin D receptor. *Mol. Endocrinol. 23*, 251−264.

(16) Rachez, C., and Freedman, L. P. (2000) Mechanisms of gene regulation by vitamin D_3 receptor: A network of coactivator interactions. *Gene 246*, 9−21.

(17) Lamblin, M., Spingarn, R., Wang, T. T., Burger, M. C., Dabbas, B., Moitessier, N., White, J. H., and Gleason, J. L. (2010) An o-aminoanilide analogue of 1α,25-dihydroxyvitamin D_3 functions as a strong vitamin D receptor antagonist. *J. Med. Chem. 53*, 7461−7465.

(18) Kato, Y., Nakano, Y., Sano, H., Tanatani, A., Kobayashi, H., Shimazawa, R., Koshino, H., Hashimoto, Y., and Nagasawa, K. (2004) Synthesis of 1α,25-dihydroxyvitamin D3−26,23-lactams (DLAMs), a novel series of 1α,25-dihydroxyvitamin D3 antagonist. *Bioorg. Med. Chem. Lett. 14*, 2579−2583.

(19) Inaba, Y., Yoshimoto, N., Sakamaki, Y., Nakabayashi, M., Ikura, T., Tamamura, H., Ito, N., Shimizu, M., and Yamamoto, K. (2009) A new class of vitamin D analogues that induce structural rearrangement of the ligand-binding pocket of the receptor. *J. Med. Chem. 52*, 1438−1449.

(20) Nakabayashi, M., Yamada, S., Yoshimoto, N., Tanaka, T., Igarashi, M., Ikura, T., Ito, N., Makishima, M., Tokiwa, H., DeLuca, H. F., and Shimizu, M. (2008) Crystal structures of rat vitamin D receptor bound to adamantyl vitamin D analogs: Structural basis for vitamin D receptor antagonism and partial agonism. *J. Med. Chem. 51*, 5320−5329.

(21) Saito, N., and Kittaka, A. (2006) Highly potent vitamin D receptor antagonists: Design, synthesis, and biological evaluation. *ChemBioChem 7*, 1479−1490.

(22) Cho, K., Uneuchi, F., Kato-Nakamura, Y., Namekawa, J., Ishizuka, S., Takenouchi, K., and Nagasawa, K. (2008) Structure-activity relationship studies on vitamin D lactam derivatives as vitamin D receptor antagonist. *Bioorg. Med. Chem. Lett. 18*, 4287−4290.

(23) Herdick, M., Steinmeyer, A., and Carlberg, C. (2000) Antagonistic action of a 25-carboxylic ester analogue of 1α,25-dihydroxyvitamin D3 is mediated by a lack of ligand-induced vitamin

D receptor interaction with coactivators. *J. Biol. Chem. 275*, 16506−16512.
(24) Ishizuka, S., Kurihara, N., Miura, D., Takenouchi, K., Cornish, J., Cundy, T., Reddy, S. V., and Roodman, G. D. (2004) Vitamin D antagonist, TEI-9647, inhibits osteoclast formation induced by 1α,25-dihydroxyvitamin D3 from pagetic bone marrow cells. *J. Steroid Biochem. Mol. Biol. 89*−*90*, 331−334.
(25) Mita, Y., Dodo, K., Noguchi-Yachide, T., Miyachi, H., Makishima, M., Hashimoto, Y., and Ishikawa, M. (2010) LXXLL peptide mimetics as inhibitors of the interaction of vitamin D receptor with coactivators. *Bioorg. Med. Chem. Lett. 20*, 1712−1717.
(26) Nandhikonda, P., Lynt, W. Z., McCallum, M. M., Ara, T., Baranowski, A. M., Yuan, N. Y., Pearson, D., Bikle, D. D., Guy, R. K., and Arnold, L. A. (2012) Discovery of the first irreversible small molecule inhibitors of the interaction between the vitamin D receptor and coactivators. *J. Med. Chem. 55*, 4640−4651.
(27) Hong, H., Kohli, K., Garabedian, M. J., and Stallcup, M. R. (1997) GRIP1, a transcriptional coactivator for the AF-2 transactivation domain of steroid, thyroid, retinoid, and vitamin D receptors. *Mol. Cell. Biol. 17*, 2735−2744.
(28) Sznaidman, M. L., Haffner, C. D., Maloney, P. R., Fivush, A., Chao, E., Goreham, D., Sierra, M. L., LeGrumelec, C., Xu, H. E., Montana, V. G., Lambert, M. H., Willson, T. M., Oliver, W. R., Jr., and Sternbach, D. D. (2003) Novel selective small molecule agonists for peroxisome proliferator-activated receptor δ (PPARδ): Synthesis and biological activity. *Bioorg. Med. Chem. Lett. 13*, 1517−1521.
(29) Harrington, L. S., Moreno, L., Reed, A., Wort, S. J., Desvergne, B., Garland, C., Zhao, L., and Mitchell, J. A. (2010) The PPARβ/δ agonist GW0742 relaxes pulmonary vessels and limits right heart hypertrophy in rats with hypoxia-induced pulmonary hypertension. *PLoS One 5*, e9526.
(30) Zarzuelo, M. J., Jimenez, R., Galindo, P., Sanchez, M., Nieto, A., Romero, M., Quintela, A. M., Lopez-Sepulveda, R., Gomez-Guzman, M., Bailon, E., Rodriguez-Gomez, I., Zarzuelo, A., Galvez, J., Tamargo, J., Perez-Vizcaino, F., and Duarte, J. (2011) Antihypertensive effects of peroxisome proliferator-activated receptor-β activation in spontaneously hypertensive rats. *Hypertension 58*, 733−743.
(31) Maria Quintela, A., Jimenez, R., Gomez-Guzman, M., Jose Zarzuelo, M., Galindo, P., Sanchez, M., Vargas, F., Cogolludo, A., Tamargo, J., Perez-Vizcaino, F., and Duarte, J. (2012) Activation of peroxisome proliferator-activated receptor-β/-δ (PPARβ/δ) prevents endothelial dysfunction in type 1 diabetic rats. *Free Radical Biol. Med. 53*, 730−741.
(32) Matsushita, Y., Ogawa, D., Wada, J., Yamamoto, N., Shikata, K., Sato, C., Tachibana, H., Toyota, N., and Makino, H. (2011) Activation of peroxisome proliferator-activated receptor δ inhibits streptozotocin-induced diabetic nephropathy through anti-inflammatory mechanisms in mice. *Diabetes 60*, 960−968.
(33) Galuppo, M., Di Paola, R., Mazzon, E., Esposito, E., Paterniti, I., Kapoor, A., Thiemermann, C., and Cuzzocrea, S. (2010) GW0742, a high affinity PPAR-β/δ agonist reduces lung inflammation induced by bleomycin instillation in mice. *Int. J. Immunopathol. Pharmacol. 23*, 1033−1046.
(34) Zingarelli, B., Piraino, G., Hake, P. W., O'Connor, M., Denenberg, A., Fan, H., and Cook, J. A. (2010) Peroxisome proliferator-activated receptor δ regulates inflammation via NF-κB signaling in polymicrobial sepsis. *Am. J. Pathol. 177*, 1834−1847.
(35) Harrington, W. W., Britt, C. S., Wilson, J. G., Milliken, N. O., Binz, J. G., Lobe, D. C., Oliver, W. R., Lewis, M. C., and Ignar, D. M. (2007) The Effect of PPARα, PPARδ, PPARγ, and PPARpan Agonists on Body Weight, Body Mass, and Serum Lipid Profiles in Diet-Induced Obese AKR/J Mice. *PPAR Res. 2007*, 97125.
(36) Bility, M. T., Devlin-Durante, M. K., Blazanin, N., Glick, A. B., Ward, J. M., Kang, B. H., Kennett, M. J., Gonzalez, F. J., and Peters, J. M. (2008) Ligand activation of peroxisome proliferator-activated receptor β/δ (PPAR β/δ) inhibits chemically induced skin tumorigenesis. *Carcinogenesis 29*, 2406−2414.
(37) Hollingshead, H. E., Killins, R. L., Borland, M. G., Girroir, E. E., Billin, A. N., Willson, T. M., Sharma, A. K., Amin, S., Gonzalez, F. J., and Peters, J. M. (2007) Peroxisome proliferator-activated receptor-β/δ (PPARβ/δ) ligands do not potentiate growth of human cancer cell lines. *Carcinogenesis 28*, 2641−2649.
(38) Marin, H. E., Peraza, M. A., Billin, A. N., Willson, T. M., Ward, J. M., Kennett, M. J., Gonzalez, F. J., and Peters, J. M. (2006) Ligand activation of peroxisome proliferator-activated receptor β inhibits colon carcinogenesis. *Cancer Res. 66*, 4394−4401.
(39) Sertznig, P., Dunlop, T., Seifert, M., Tilgen, W., and Reichrath, J. (2009) Cross-talk between vitamin D receptor (VDR)- and peroxisome proliferator-activated receptor (PPAR)-signaling in melanoma cells. *Anticancer Res. 29*, 3647−3658.
(40) Boehm, M. F., Fitzgerald, P., Zou, A., Elgort, M. G., Bischoff, E. D., Mere, L., Mais, D. E., Bissonnette, R. P., Heyman, R. A., Nadzan, A. M., Reichman, M., and Allegretto, E. A. (1999) Novel nonsecosteroidal vitamin D mimics exert VDR-modulating activities with less calcium mobilization than 1,25-dihydroxyvitamin D3. *Chem. Biol. 6*, 265−275.
(41) Teichert, A., Arnold, L. A., Otieno, S., Oda, Y., Augustinaite, I., Geistlinger, T. R., Kriwacki, R. W., Guy, R. K., and Bikle, D. D. (2009) Quantification of the vitamin D receptor-coregulator interaction. *Biochemistry 48*, 1454−1461.
(42) Rochel, N., Wurtz, J. M., Mitschler, A., Klaholz, B., and Moras, D. (2000) The crystal structure of the nuclear receptor for vitamin D bound to its natural ligand. *Mol. Cell 5*, 173−179.
(43) Hwang, J. Y., Huang, W. W., Arnold, L. A., Huang, R. L., Attia, R. R., Connelly, M., Wichterman, J., Zhu, F. Y., Augustinaite, I., Austin, C. P., Inglese, J., Johnson, R. L., and Guy, R. K. (2011) Methylsulfonylnitrobenzoates, a New Class of Irreversible Inhibitors of the Interaction of the Thyroid Hormone Receptor and Its Obligate Coactivators That Functionally Antagonizes Thyroid Hormone. *J. Biol. Chem. 286*, 11895−11908.
(44) Estebanez-Perpina, E., Arnold, L. A., Jouravel, N., Togashi, M., Blethrow, J., Mar, E., Nguyen, P., Phillips, K. J., Baxter, J. D., Webb, P., Guy, R. K., and Fletterick, R. J. (2007) Structural insight into the mode of action of a direct inhibitor of coregulator binding to the thyroid hormone receptor. *Mol. Endocrinol. 21*, 2919−2928.
(45) Rachez, C., Suldan, Z., Ward, J., Chang, C. P., Burakov, D., Erdjument-Bromage, H., Tempst, P., and Freedman, L. P. (1998) A novel protein complex that interacts with the vitamin D3 receptor in a ligand-dependent manner and enhances VDR transactivation in a cell-free system. *Genes Dev. 12*, 1787−1800.
(46) Horoszewicz, J. S., Leong, S. S., Kawinski, E., Karr, J. P., Rosenthal, H., Chu, T. M., Mirand, E. A., and Murphy, G. P. (1983) LNCaP model of human prostatic carcinoma. *Cancer Res. 43*, 1809−1818.
(47) Mueller, E., Smith, M., Sarraf, P., Kroll, T., Aiyer, A., Kaufman, D. S., Oh, W., Demetri, G., Figg, W. D., Zhou, X. P., Eng, C., Spiegelman, B. M., and Kantoff, P. W. (2000) Effects of ligand activation of peroxisome proliferator-activated receptor γ in human prostate cancer. *Proc. Natl. Acad. Sci. U.S.A. 97*, 10990−10995.
(48) Hsieh, M. L., and Juang, H. H. (2005) Cell growth effects of triiodothyronine and expression of thyroid hormone receptor in prostate carcinoma cells. *J. Androl. 26*, 422−428.
(49) Skowronski, R. J., Peehl, D. M., and Feldman, D. (1993) Vitamin D and prostate cancer: 1,25-Dihydroxyvitamin D3 receptors and actions in human prostate cancer cell lines. *Endocrinology 132*, 1952−1960.
(50) Linja, M. J., Porkka, K. P., Kang, Z., Savinainen, K. J., Janne, O. A., Tammela, T. L., Vessella, R. L., Palvimo, J. J., and Visakorpi, T. (2004) Expression of androgen receptor coregulators in prostate cancer. *Clin. Cancer Res. 10*, 1032−1040.
(51) Vijayvargia, R., May, M. S., and Fondell, J. D. (2007) A coregulatory role for the mediator complex in prostate cancer cell proliferation and gene expression. *Cancer Res. 67*, 4034−4041.
(52) Takayama, K., Kaneshiro, K., Tsutsumi, S., Horie-Inoue, K., Ikeda, K., Urano, T., Ijichi, N., Ouchi, Y., Shirahige, K., Aburatani, H., and Inoue, S. (2007) Identification of novel androgen response genes in prostate cancer cells by coupling chromatin immunoprecipitation and genomic microarray analysis. *Oncogene 26*, 4453−4463.

(53) Riegman, P. H., Vlietstra, R. J., van der Korput, J. A., Brinkmann, A. O., and Trapman, J. (1991) The promoter of the prostate-specific antigen gene contains a functional androgen responsive element. *Mol. Endocrinol. 5*, 1921−1930.
(54) Mandard, S., Zandbergen, F., Tan, N. S., Escher, P., Patsouris, D., Koenig, W., Kleemann, R., Bakker, A., Veenman, F., Wahli, W., Muller, M., and Kersten, S. (2004) The direct peroxisome proliferator-activated receptor target fasting-induced adipose factor (FIAF/PGAR/ANGPTL4) is present in blood plasma as a truncated protein that is increased by fenofibrate treatment. *J. Biol. Chem. 279*, 34411−34420.
(55) Tsui, K. H., Hsieh, W. C., Lin, M. H., Chang, P. L., and Juang, H. H. (2008) Triiodothyronine modulates cell proliferation of human prostatic carcinoma cells by downregulation of the B-cell translocation gene 2. *Prostate 68*, 610−619.
(56) Colston, K. W., Perks, C. M., Xie, S. P., and Holly, J. M. (1998) Growth inhibition of both MCF-7 and Hs578T human breast cancer cell lines by vitamin D analogues is associated with increased expression of insulin-like growth factor binding protein-3. *J. Mol. Endocrinol. 20*, 157−162.
(57) Peng, L., Malloy, P. J., and Feldman, D. (2004) Identification of a functional vitamin D response element in the human insulin-like growth factor binding protein-3 promoter. *Mol. Endocrinol. 18*, 1109−1119.
(58) Hoenderop, J. G., van der Kemp, A. W., Hartog, A., van de Graaf, S. F., van Os, C. H., Willems, P. H., and Bindels, R. J. (1999) Molecular identification of the apical Ca^{2+} channel in 1, 25-dihydroxyvitamin D3-responsive epithelia. *J. Biol. Chem. 274*, 8375−8378.
(59) Meyer, M. B., Watanuki, M., Kim, S., Shevde, N. K., and Pike, J. W. (2006) The human transient receptor potential vanilloid type 6 distal promoter contains multiple vitamin D receptor binding sites that mediate activation by 1,25-dihydroxyvitamin D3 in intestinal cells. *Mol. Endocrinol. 20*, 1447−1461.
(60) Chen, K. S., and DeLuca, H. F. (1995) Cloning of the human 1α,25-dihydroxyvitamin D-3 24-hydroxylase gene promoter and identification of two vitamin D-responsive elements. *Biochim. Biophys. Acta 1263*, 1−9.
(61) Miyaura, C., Abe, E., Kuribayashi, T., Tanaka, H., Konno, K., Nishii, Y., and Suda, T. (1981) 1α,25-Dihydroxyvitamin D3 induces differentiation of human myeloid leukemia cells. *Biochem. Biophys. Res. Commun. 102*, 937−943.
(62) Mangelsdorf, D. J., Koeffler, H. P., Donaldson, C. A., Pike, J. W., and Haussler, M. R. (1984) 1,25-Dihydroxyvitamin D3-induced differentiation in a human promyelocytic leukemia cell line (HL-60): Receptor-mediated maturation to macrophage-like cells. *J. Cell Biol. 98*, 391−398.
(63) Collins, S. J., Ruscetti, F. W., Gallagher, R. E., and Gallo, R. C. (1979) Normal functional characteristics of cultured human promyelocytic leukemia cells (HL-60) after induction of differentiation by dimethylsulfoxide. *J. Exp. Med. 149*, 969−974.
(64) Wang, Y., Chirgadze, N. Y., Briggs, S. L., Khan, S., Jensen, E. V., and Burris, T. P. (2006) A second binding site for hydroxytamoxifen within the coactivator-binding groove of estrogen receptor β. *Proc. Natl. Acad. Sci. U.S.A. 103*, 9908−9911.
(65) Kojetin, D. J., Burris, T. P., Jensen, E. V., and Khan, S. A. (2008) Implications of the binding of tamoxifen to the coactivator recognition site of the estrogen receptor. *Endocr.-Relat. Cancer 15*, 851−870.
(66) Xu, H. E., Lambert, M. H., Montana, V. G., Plunket, K. D., Moore, L. B., Collins, J. L., Oplinger, J. A., Kliewer, S. A., Gampe, R. T., Jr., McKee, D. D., Moore, J. T., and Willson, T. M. (2001) Structural determinants of ligand binding selectivity between the peroxisome proliferator-activated receptors. *Proc. Natl. Acad. Sci. U.S.A. 98*, 13919−13924.
(67) Han, V. K., Bassett, N., Walton, J., and Challis, J. R. (1996) The expression of insulin-like growth factor (IGF) and IGF-binding protein (IGFBP) genes in the human placenta and membranes: Evidence for IGF-IGFBP interactions at the feto-maternal interface. *J. Clin. Endocrinol. Metab. 81*, 2680−2693.
(68) Khanim, F. L., Gommersall, L. M., Wood, V. H., Smith, K. L., Montalvo, L., O'Neill, L. P., Xu, Y., Peehl, D. M., Stewart, P. M., Turner, B. M., and Campbell, M. J. (2004) Altered SMRT levels disrupt vitamin D3 receptor signalling in prostate cancer cells. *Oncogene 23*, 6712−6725.
(69) Canzoniere, D., Farioli-Vecchioli, S., Conti, F., Ciotti, M. T., Tata, A. M., Augusti-Tocco, G., Mattei, E., Lakshmana, M. K., Krizhanovsky, V., Reeves, S. A., Giovannoni, R., Castano, F., Servadio, A., Ben-Arie, N., and Tirone, F. (2004) Dual control of neurogenesis by PC3 through cell cycle inhibition and induction of Math1. *J. Neurosci. 24*, 3355−3369.
(70) Aronsson, L., Huang, Y., Parini, P., Korach-Andre, M., Hakansson, J., Gustafsson, J. A., Pettersson, S., Arulampalam, V., and Rafter, J. (2010) Decreased fat storage by *Lactobacillus paracasei* is associated with increased levels of angiopoietin-like 4 protein (ANGPTL4). *PLoS One 5*, e13087.
(71) Carlberg, C., Molnar, F., and Mourino, A. (2012) Vitamin D receptor ligands: The impact of crystal structures. *Expert Opin. Ther. Pat. 22*, 417−435.